

Javier Rico (for the MAGIC Collaboration)

Results from MAGIC's first observation cycle on galactic sources

Received: date / Accepted: date

Abstract During its Cycle I, the MAGIC telescope targeted about 250 hours several galactic sources sought to be, or detected previously by other experiments in the same energy domain, γ -ray emitters. This paper reviews some results of such MAGIC observations covering, among others, supernova remnants, the Galactic Center and microquasars. We will concentrate on the recent discovery at very high energy γ -rays of the microquasar LS I +61 303.

Keywords γ -ray astronomy · Galactic objects · Microquasars · LS I +61 303

PACS 98.70.Rz · 97.80.Jp · 95.85.-e · 95.85.Pw

1 Introduction: The MAGIC Telescope

MAGIC is a telescope for very high energy (VHE, $E \geq 50 - 100$ GeV) γ -ray observation exploiting the Imaging Air Cherenkov (IAC) technique. It is located on the Roque de los Muchachos Observatory ($28^{\circ}45'30''N$, $17^{\circ}52'48''W$, 2250 m above sea level) in La Palma (Spain). This kind of instrument images the Cherenkov light produced in the particle cascade initiated by a γ -ray in the atmosphere. MAGIC incorporates a number of technological improvements in its design and is currently the largest single-dish telescope (diameter 17 m) in this energy band, yielding the lowest threshold (~ 50 GeV). It is equipped with a 576-pixel photomultiplier camera with a 3.5° field of view. MAGIC's sensitivity above 100 GeV is $\sim 2.5\%$ of the Crab nebula flux (the calibration standard candle for IAC telescopes) in 50 hours of observations. The energy resolution above 200 GeV is better than 30%. The angular resolution is $\sim 0.1^{\circ}$, while source

localization in the sky is provided with a precision of $\sim 2'$. MAGIC is also unique among IAC telescopes by its capability to operate under moderate illumination (i.e. moonlight and twilight). This allows to increase the duty cycle by a factor 1.5 and a better sampling of variable sources is possible.

The physics program developed with the MAGIC telescope includes both, topics of fundamental physics and astrophysics. In this paper we present the results regarding the observations of galactic targets. The results from extragalactic observations are presented elsewhere in these proceedings [1].

2 Highlights of cycle I

MAGIC's first observation cycle spanned the period from January 2005 to April 2006. About 1/4 of the observation time (not counting that devoted to Crab nebula technical observations) was devoted to galactic objects. The observations covered both, candidates and well established VHE γ -ray emitters, and included the following types of objects: supernova remnants (SNRs), pulsars, pulsar wind nebulae (PWN), microquasars (μ QSRs), the Galactic Center (GC), one unidentified TeV source and one cataclysmic variable. In this section we highlight the results obtained so far from such observations, and concentrate, in section 3, on the most interesting case of the microquasar LS I +61 303.

2.1 The Crab nebula and pulsar

The Crab nebula is a steady emitter at GeV and TeV energies, what makes it into an excellent calibration candle. The Crab nebula has been observed extensively in the past over a wide range of wavelengths, covering the radio, optical and x-ray bands, as well as high-energy regions up to nearly 100 TeV. Nevertheless, some of the relevant physics phenomena are expected to happen in

Javier Rico
Institut de Física d'Altes Energies
Edifici Cn Universitat Autònoma de Barcelona
08193 Bellaterra (Barcelona) Spain
Tel.: +34 93 581 3551
Fax: +34 93 581 1938
E-mail: jrico@ifae.es

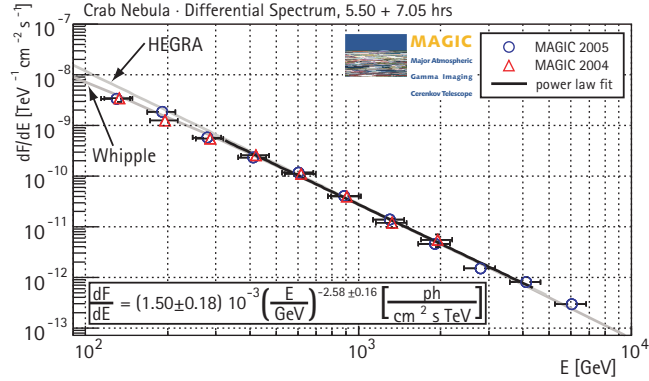


Fig. 1 Energy spectrum above 100 GeV from the Crab nebula measured by MAGIC in two different observation seasons. For comparison, the extrapolations down to 100 of HEGRA and Whipple measurements are shown.

Table 1 Upper limits (UL) to the pulsed integral flux from three pulsars observed by MAGIC. The considered energy threshold (E_{th}), observation time (OT), assumed duty cycle (DC) and confidence level (CL) are also shown.

Pulsar	E_{th} [GeV]	OT [hour]	DC (%)	CL (%)	UL [ph s ⁻¹ cm ⁻²]
Crab	90	4	21	95	2.0×10^{-10}
Crab	150	4	21	95	1.1×10^{-10}
PSR B1957+20	115	6	5	90	2.9×10^{-11}
PSR J0218+4232	115	24	5	90	1.1×10^{-10}

the VHE domain, namely the spectrum showing an inverse Compton (IC) peak close to 100 GeV, a cut-off of the pulsed emission somewhere between 10 and 100 GeV, and the verification of the flux stability down to the percent level. The existing VHE γ -ray experimental data is very well described by electron acceleration followed by the IC scattering of photons generated by synchrotron radiation (synchrotron self Compton process). Probing the presence/absence of a small contribution of VHE γ 's produced in hadronic interactions is a challenge for experimenters.

Along the first cycle of MAGIC's regular observations, a significant amount of time has been devoted to observe the Crab nebula, both for technical and astrophysical studies. The performance of the telescope has been experimentally evaluated and found in good agreement with the expectations and Monte Carlo simulations [2, 3]. This has allowed us to perform routine analyses above 100 GeV, where the performance of our instrument is fully understood. On the other hand, a sample of 12 hours of selected data has been used to measure with high precision the spectrum down to ~ 100 GeV, as shown in figure 1 [2]. We have also carried out a search for pulsed γ -ray emission from Crab pulsar and two millisecond pulsars [4, 5], albeit without positive result. The derived upper limits of the pulsed flux for the three observed pulsars are shown in Table 1.

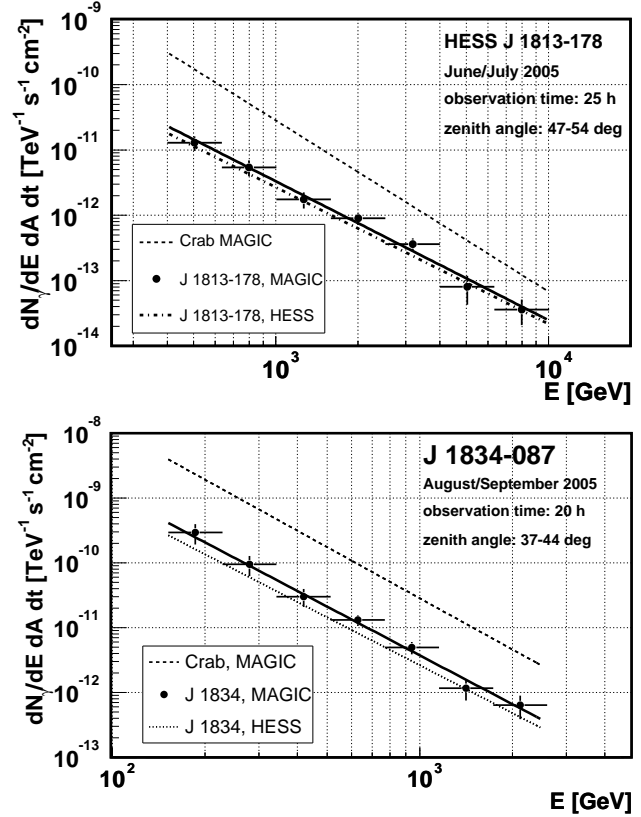


Fig. 2 Energy spectrum above 400 GeV of HESS J1813-178 (top) and above 150 GeV of HESS J1834-087 (bottom), measured by MAGIC. For comparison, also the spectra measured by HESS and that of the Crab nebula are shown.

2.2 Supernova Remnants

Shocks produced at supernova explosions are assumed to be the source of the galactic component of the cosmic ray flux [6]. The proof that this is the case could be provided by observations in the VHE domain. The rationale is that the hadronic component of the cosmic rays –enhanced close to their source, i.e. the SNR– should produce VHE γ -rays by the interaction with nearby dense molecular clouds. Although recent data seem to indicate that this is the case, it is difficult to disentangle the VHE component initiated by hadrons from that produced by Bremsstrahlung and IC processes by accelerated electrons. Therefore more data in the TeV regime together with multi-wavelength studies are needed to finally solve the long-standing puzzle of the origin of galactic cosmic rays.

Within its program of observation of galactic sources, MAGIC has observed a number of supernova remnants. In particular, we are observing several of the brightest EGRET sources associated to SNRs, and the analysis of the acquired data is in progress. On the other hand, we have confirmed the VHE γ -ray emission from the SNRs HESS J1813-178 [7] and HESS J1834-087 (W41) [8]. Our

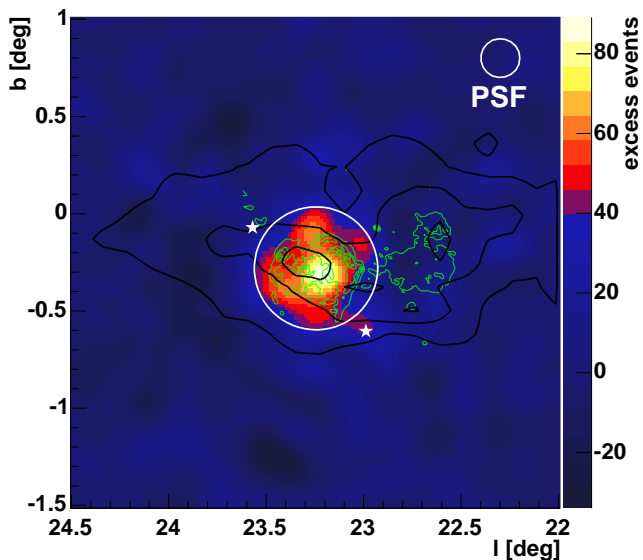


Fig. 3 Sky map of γ -ray candidate events (background subtracted) in the direction of HESS J1834-087 for an energy threshold of about 250 GeV. Overlaid are ^{12}CO emission contours (black) [9] and contours of 90 cm VLA radio data (green) [10].

results have confirmed SNRs as a well established population of VHE γ -ray emitters. The energy spectra measured by MAGIC for these two sources are shown in Figure 2. They are, both, well described by an unbroken power law and an intensity of about 10% of the Crab nebula flux. Furthermore, MAGIC has proven its capability to study moderately extended sources by observing HESS J1834-087. The morphology of this object measured by MAGIC is shown in Figure 3. Interestingly, the maximum of the VHE emission has been correlated with a maximum in the density of a nearby molecular cloud (shown in the figure by the contour lines of the ^{12}CO emission intensities). Although the mechanism responsible for the VHE radiation remains yet to be clarified, this is a hint that it could be produced by high energy hadrons interacting with the molecular cloud.

2.3 Galactic Center

We have also measured the VHE γ -ray flux from the GC [11]. The possibility to indirectly detect dark matter through its annihilation into VHE γ -rays has risen the interest to observe this region during the last years. Our observations have confirmed a point-like γ -ray excess whose location is spatially consistent with Sgr A* as well as Sgr A East. The energy spectrum of the detected emission is well described by an unbroken power law of photon index $\alpha = -2.2$ and intensity about 10% of that of the Crab nebula flux at 1 TeV. This result disfavours dark matter annihilation as the main origin

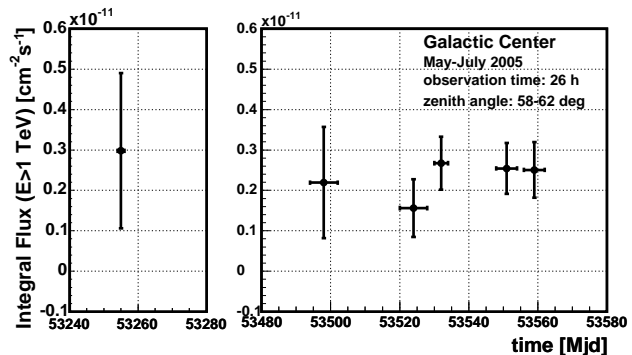


Fig. 4 Integral VHE γ -ray flux above 1 TeV as a function of time from the GC as measured by MAGIC during September 2004 and May-July 2005.

of the detected flux. Furthermore, there is no evidence for variability of the flux on hour/day time scales nor on a year scale, as shown in Figure 4. This suggests that the acceleration takes place in a steady object such as a SNR or a PWN, and not in the central black hole.

2.4 Other observation targets

MAGIC observation program of galactic sources includes also other kinds of objects such as PWN, cataclysmic variables, unidentified sources and μQSRs (both high and low mass). The analyses regarding these sources are ongoing and will be reported in the near future. The one exception is the high-mass x-ray binary LS I +61 303, discussed in the section 3.

3 The microquasar LS I +61 303

3.1 Microquasars

Microquasars are a subclass of stellar, x-ray binary systems that display prominent radio emission, usually attributed to the existence of jets of relativistic particles. They are named after the similarities with active galactic nuclei (AGNs), since μQSRs show the same three ingredients that make up radio-loud AGNs: a compact object, an accretion disc, and relativistic jets [12]. Hence, μQSRs are galactic, scaled-down versions of an AGN, where instead of a super-massive black hole we deal with a compact object of just a few solar masses that accretes material from a donor star. The similarities with AGNs explain the large interest risen by μQSRs . Crucial for our understanding of accreting systems is also that: (i) μQSRs are nearby objects, and (ii) they show very short timescale variability. Those reasons make these objects ideal laboratories for the study of the physical processes that govern how μQSRs and AGNs work. In particular,

the short timescale variability displayed by μ QSRs allows to see changes in the ongoing physical processes within typical time scales ranging from minutes to months, in contrast with the usual scales of years to observe such variability in AGNs. In addition, μ QSRs could measurably contribute to the density of galactic cosmic rays [13].

3.2 LS I +61 303

One of the most studied μ QSR candidates is LS I +61 303. This system is composed of a compact object of unknown nature (neutron star or black hole) in a highly eccentric ($e = 0.7$) orbit around a Be star. The orbital period – with associated radio [14] and x-ray [15] outbursts – is 26.5 days and periastron passage is at phase 0.23 [16]. The phase and intensity of the radio outburst show a modulation of 4.6 years [17]. High-resolution radio imaging techniques have shown extended, radio-emitting structures with angular extension of ~ 0.01 to ~ 0.1 arc-sec, interpreted within the framework of μ QSR scenario, where the radio emission is originated in a two-sided, probably precessing, relativistic jet ($\beta/c = 0.6$) [18]. However, no solid evidence of the presence of an accretion disk (i.e. a thermal x-ray component) has been observed. LS I +61 303 is also one of the two μ QSR candidates positionally coincident with EGRET γ -ray sources [19], and the only one located in the Northern Hemisphere –hence a suitable target for MAGIC. There are also hints of variability of the γ -ray flux [20]. However, the large uncertainty of the position of the EGRET source has not allowed an unambiguous association with LS I +61 303.

3.3 MAGIC observations

LS I +61 303 was observed in the VHE regime with MAGIC during 54 hours (after standard quality selection, discarding bad weather data) between October 2005 and March 2006 [21]. The data analysis was carried out using the standard MAGIC reconstruction and analysis software [7,8,11].

Figure 5 shows the reconstructed γ -ray map during two different observation periods, around periastron passage and at higher (0.4-0.7) orbital phases. No significant excess in the number of γ -ray events is detected around periastron passage, whereas it shows up clearly (9.4σ statistical significance) at later orbital phases. The distribution of γ -ray excess is consistent with a point-like source and is located at (J2000): $\alpha = 2^{\text{h}}40^{\text{m}}34^{\text{s}}$, $\delta = 61^{\circ}15'25''$, with statistical and systematic uncertainties of $\pm 0.4'$ and $\pm 2'$, respectively, in agreement with the position of LS I +61 303. In the natural case in which the VHE emission is produced by the same object detected at EGRET energies, this result identifies a γ -ray source that resisted classification during the last three decades.

Our measurements show that the VHE γ -ray emission from LS I +61 303 is variable. The γ -ray flux above

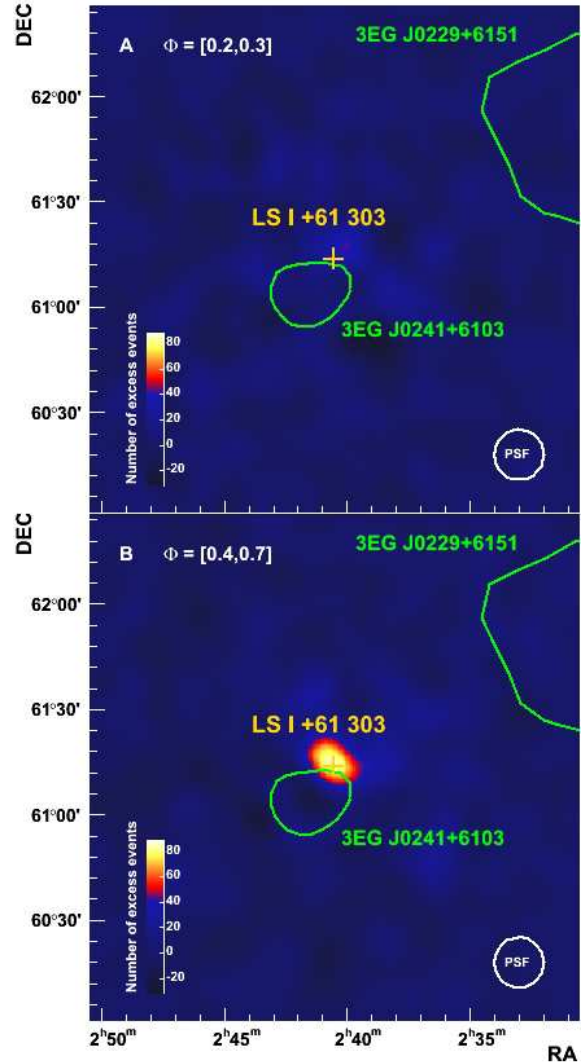


Fig. 5 Smoothed maps of γ -ray excess events above 400 GeV around LS I +61 303. (A) Observations over 15.5 hours corresponding to data around periastron (i.e., between orbital phases 0.2 and 0.3). (B) Observations over 10.7 hours at orbital phase between 0.4 and 0.7. The number of events is normalized in both cases to 10.7 hours of observation. The position of the optical source LS I +61 303 (yellow cross) and the 95% confidence level contours for the EGRET sources 3EG J0229+6151 and 3EG J0241+6103 (green contours) are also shown. The bottom right circle shows the size of the point spread function of MAGIC (1σ radius). From Albert *et al.* [21].

400 GeV coming from the direction of LS I +61 303 (see Figure 6) has a maximum corresponding to about 16% of the Crab nebula flux, and is detected at around phase 0.6. The combined statistical significance of the 3 highest flux measurements is 8.7σ , for an integrated observation time of 4.2 hours. The probability for the distribution of measured fluxes to be a statistical fluctuation of a constant flux (obtained from a χ^2 fit of a constant function to the entire data sample) is 3×10^{-5} . The fact that the detections occur at similar orbital phases hints at a

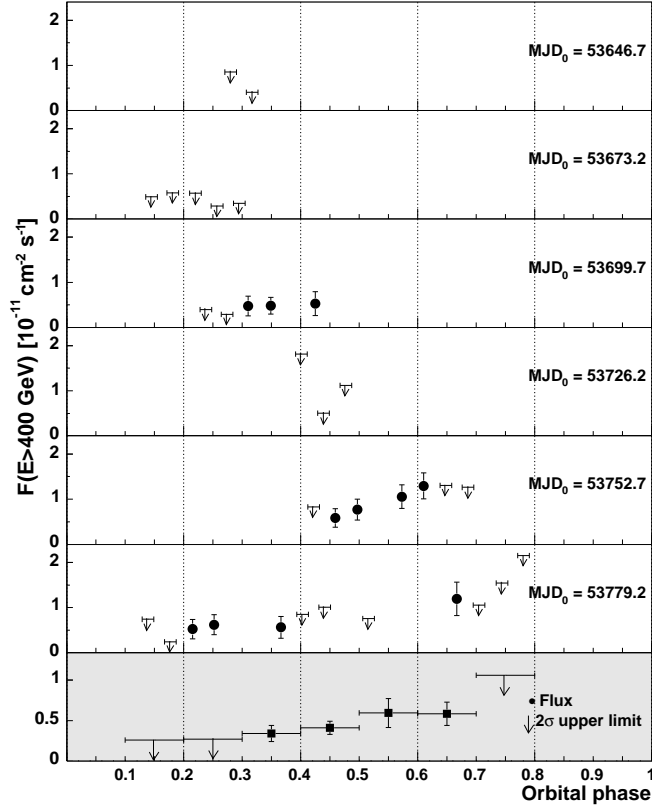


Fig. 6 VHE γ -ray flux of LS I +61 303 as a function of orbital phase for the six observed orbital cycles (six upper panels, one point per observation night) and averaged for the entire observation time (bottom panel). Vertical error bars include 1σ statistical error and 10% systematic uncertainty on day-to-day relative fluxes. Only data points with more than 2σ significance are shown, and 2σ upper limits [22] are derived for the rest. The modified Julian date (MJD) corresponding to orbital phase 0 is indicated for every orbital cycle. From Albert *et al.* [21].

periodic nature of the VHE γ -ray emission. Contemporaneous radio observations of LS I +61 303 were carried out at 15 GHz with the Ryle Telescope covering several orbital periods of the source. The peak of the radio outbursts was at phase 0.7, i.e. between 1 and 3 days after the increase observed at VHE γ -rays flux (see Figure 7).

The VHE spectrum derived from data between ~ 200 GeV and ~ 4 TeV at orbital phases between 0.4 and 0.7 (see Figure 8) is fitted reasonably well ($\chi^2/ndf = 6.6/5$) by a power law function:

$$dN/(dA/dt/dE) = (2.7 \pm 0.4 \pm 0.8) \times 10^{-12} \times E^{(-2.6 \pm 0.2 \pm 0.2)} \text{ cm}^{-2} \text{ s}^{-1} \text{ TeV}^{-1} \quad (1)$$

where N is the number of γ -rays reaching Earth per unit area A , time t and energy E (expressed in TeV). Errors quoted are statistical and systematic, respectively. This spectrum is consistent with that measured by EGRET for a spectral break between 10 and 100 GeV. The flux from LS I +61 303 above 200 GeV corresponds to an

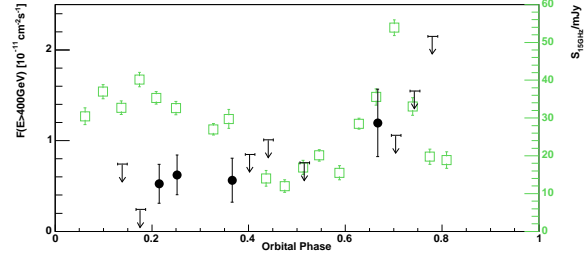


Fig. 7 LS I +61 303 radio flux density at 15 GHz measured with the Ryle Telescope (green squares, right axis) and results from the last orbital cycle observed by MAGIC (black dots, left axis), from 14 February to 8 March 2006. The MJD corresponding to orbital phase 0 is indicated. From Albert *et al.* [21].

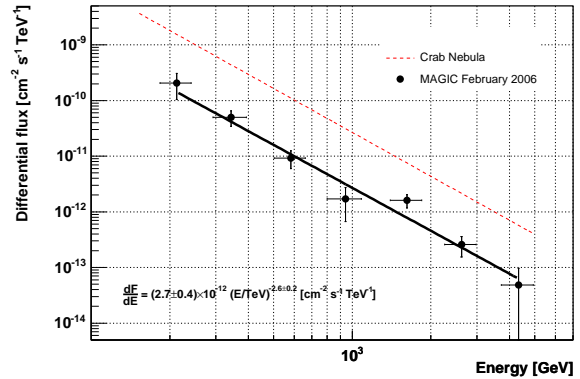


Fig. 8 Differential energy spectrum of LS I +61 303 for energies between 200 GeV and 4 TeV and averaged for orbital phases between 0.4 and 0.7, measured by MAGIC. The error bars show the 1σ statistical uncertainty. The dashed, red line corresponds to the Crab nebula differential spectrum also measured by MAGIC. The solid, black line is a fit of a power law (also expressed mathematically in the inset) to the measured points. From Albert *et al.* [21].

isotropic luminosity of $\sim 7 \times 10^{33} \text{ erg s}^{-1}$ (assuming a distance to the system of 2 kpc [23]), of the same order of that of the similar object LS 5039 [24], and a factor ~ 2 lower than the previous experimental upper limit ($< 8.8 \times 10^{-12} \text{ cm}^{-2} \text{ s}^{-1}$ above 500 GeV) [25]. LS I +61 303 displays more luminosity at GeV than at x-ray energies, a behavior shared also by LS 5039.

3.4 Emission scenarios

LS I +61 303 belongs, together with LS 5039 [24] and PSR B1259-63 [26], to a new class of objects, the so-called γ -ray binary systems, whose electromagnetic emission extends up to the TeV domain. LS I +61 303 and LS 5039 are usually thought to be μ QSRs, since evidences of relativistic jets have been found at radio frequencies. In such scenario, the high energy emission is

produced by the shocks triggered at the relativistic jets [12]. However, no clear signal of the presence of an accretion disk (in particular an spectral feature between ~ 10 and ~ 100 keV due to the cut-off of the thermal emission) has been observed so far. Because of that, it has been alternatively proposed that relativistic particles could be injected into the surrounding medium by the wind from a young pulsar [27], which seems to be the case of PSR B1259-63. In the case of LS I +61 303 also the resemblance of the time variability and the radio/x-ray spectra with those of young pulsars seem to support such hypothesis. However, no pulsed emission has been detected from LS I +61 303. Therefore, the existing data in the radio/x/ γ -ray domain, cannot conclusively confirm, or rule out, none of the two proposed scenarios. Thus, the question of whether the three known γ -ray binaries produce TeV emission by the same mechanism, and by which one, is currently object of an intense debate [28]. Observation at VHE with MAGIC simultaneously together with other instruments at other wavelength domains –in particular radio– will help elucidate the mechanism of the TeV emission and hence the nature of γ -ray binaries.

The observation of jets has triggered the study of different microquasar-based γ -ray emission models, some regarding hadronic mechanisms: relativistic protons in the jet interact with non-relativistic stellar wind ions, producing γ -rays via neutral pion decay [29]; some regarding leptonic mechanisms: IC scattering of relativistic electrons in the jet on stellar and/or synchrotron photons [30].

The TeV flux measured by MAGIC has a maximum at phases 0.5-0.6 (see Figure 6), overlapping with the x-ray outburst and the onset of the radio outburst. The timescale of the TeV variability constrains the emitting region to be smaller than a few 10^{15} cm (or 0.1 arc-sec at 2 kpc), which is larger than the binary system and of the same order of the detected radio jet-like structures. The maximum flux is not detected at periastron, when the accretion rate is expected to be the largest. This result seems to favor the leptonic over the hadronic models, since the IC efficiency is likely to be higher than that of proton-proton collisions at the relatively large distances from the companion star at this orbital phase. Further, VHE γ -ray emission that peaks after periastron passage has been predicted considering electromagnetic cascading within the binary system [31]. It is also possible to explain the orbital modulation of the VHE emission in LS I +61 303 by the geometrical effect of changes in the relative orientation of the stellar companion with respect to the compact object and jet as it impacts the position and depth of the $\gamma\gamma$ absorption trough [32]. The existing data are, however, not conclusive to confirm or rule out any of the theoretical models existing in the literature. Concerning energetics, a relativistic power of several 10^{35} erg s $^{-1}$, extracted from accretion, could explain

the non thermal luminosity of the source from radio to VHE γ -rays.

LS I +61 303 is an excellent laboratory to study the VHE γ -ray emission and absorption processes taking place in massive x-ray binaries: the high eccentricity of the binary system provides very different physical conditions to be tested on timescales of less than one month. Future MAGIC observations will test both, the periodicity of the signal and its intra-night variability.

Acknowledgements. We thank the Instituto de Astrofísica de Canarias for the excellent working conditions at the Observatorio Roque de los Muchachos in La Palma

References

1. Mazin, D.: These proceedings.
2. Wagner, R. *et al.*: Proceedings of the 29th International Cosmic Ray Conference, Pune (India) 3-11 Aug 2005, Vol. 4, 163-166.
3. Cortina, J. *et al.*: Proceedings of the 29th International Cosmic Ray Conference, Pune (India) 3-11 Aug 2005, Vol. 5, 359-362.
4. López, M.: J. Phys.: Conf. Ser. **39** 485-485 (2006).
5. Oña-Wilhelmi, E. *et al.*: Proceedings of the 29th International Cosmic Ray Conference, Pune (India) 3-11 Aug 2005, Vol. 4, 247 - 250.
6. Baade, W. and Zwicky, F.: Phys. Rev. **45** 138 (1934).
7. Albert, J. *et al.*: Astrophys. J. **637** L41-L44 (2006).
8. Albert, J. *et al.*, Astrophys. J. **643** L53-L56 (2006).
9. Dame, T. M., Hartmann, D. and Thaddeus, P.: Astrophys. J. **547** 792-813 (2001).
10. White, R. L., Becker, R. H. and Helfand, D. J.: Astron. J. **130** 586-596. (2005).
11. Albert, J. *et al.*: Astrophys. J.: **638**, L101-L104 (2006).
12. Mirabel, I. F. and Rodríguez, L. F.: Annual Review of Astronomy and Astrophysics **37**, 409-443 (1999).
13. Heinz, S. and Sunyaev, R. A.: Astron. Astrophys. **390**, 751-766 (2002).
14. Gregory, P. C., Taylor, A. R.: Nature **272**, 704-706 (1978).
15. Taylor, A. R. *et al.*: Astron. Astrophys. **305**, 817-824 (1996).
16. Casares, J. *et al.*: Mon. Not. R. Astron. Soc. **360**, 1105-1109 (2005).
17. Gregory, P. C.: Astrophys. J. **575**, 427-434 (2002).
18. Massi, M. *et al.*: Astron. Astrophys. **414**, L1-L4 (2004).
19. Kniffen D. A. *et al.*: Astrophys. J. **486**, 126-131 (1997).
20. Tavani, M. *et al.*: Astrophys. J. **497**, L89-L91 (1998).
21. Albert, J. *et al.*: Science **312**, 1771-1773 (2006).
22. Rolke, W. A. *et al.*: Nucl. Inst. Meth. **A551**, 493-503 (2005).
23. Fraail, D. A. and Hjellming, R. M.: Astron. J. **101** 2126-2130 (1991).
24. de Naurois, M.: These proceedings.
25. Fegan S. J. *et al.*: Astrophys. J. **624**, 638-655 (2005).
26. Aharonian, F. *et al.*: Astron. Astrophys. **442** 1-10 (2005).
27. Maraschi, L. and Treves, A.: Mon. Not. R. Astron. Soc. **194**, 1P (1981).
28. Mirabel, F.: Science **312** 1759-1760 (2006).
29. Romero, G. E.: These proceedings.
30. Bosch-Ramon, V., Romero, G. E., Paredes, J. M.: Astron. Astrophys. **447**, 263-276 (2006).
31. Bednarek, W.: Mon. Not. R. Astron. Soc. **368**, 579-591 (2006).
32. Gupta, S. and Boettcher, M.: astro-ph/0606590.